

Microarray analysis of differential gene expression in temporomandibular joint condylar cartilage after experimentally induced osteoarthritis

Juanhong Meng D.D.S., Ph.D.†, Xuchen Ma D.D.S., Ph.D.†*,

Dalong Ma Ph.D.‡ and Cairmin Xu B.Sc.§

† Center for TMD & Orofacial Pain, School of Stomatology, Peking University, Beijing 100081, PR China

‡ Center of Human Disease Gene Research, Peking University, Beijing 100083, PR China

§ National Laboratory of Medical Molecular Biology, Institute of Basic Medical Sciences, Chinese Academy of Medical Sciences and Peking Union Medical College, Beijing 100005, PR China

Summary

Objective: To identify the gene expression profile of mandibular condylar cartilage after experimentally induced osteoarthritis (OA).

Design: We studied the gene expression levels in temporomandibular joint (TMJ) condylar cartilage during different stages of experimentally induced OA. The pathological characteristics of normal, early-stage and late-stage osteoarthritic TMJ cartilage were verified by histological techniques. The gene expression profiles in normal and osteoarthritic cartilage were measured by Affymetrix RAE230A microarrays. Some of the gene transcripts were confirmed by quantitative real-time reverse-transcription PCR analysis.

Results: A comprehensive, differentially expressed, gene profile was obtained in TMJ cartilage during the progression of OA. In total, 138 genes and expressed sequence tags were up- or down-regulated at least 2-fold. Some of these genes have been shown to play a role in OA, including matrix-degrading proteases, protease inhibitors and genes involved in cell growth, apoptosis and bone remodeling. However, some genes that had never been reported to be related with OA, such as AQP3, SPP2, NOV, DKK3 and EGLN3, were consistently observed to be up-regulated in this study, suggesting they may be involved in OA progression.

Conclusion: This study provides a new gene expression profile of the progression of OA. Further study of these OA-related genes may provide new insights into understanding the molecular mechanisms underlying OA.

© 2005 OsteoArthritis Research Society International. Published by Elsevier Ltd. All rights reserved.

Key words: Osteoarthritis, Temporomandibular joint, Cartilage, Differentially expressed gene, Microarray.

Introduction

Osteoarthritis (OA) results from an imbalance between chondrocyte-controlled anabolic and catabolic processes, and is characterized by progressive degradation of components of the extracellular matrix (ECM) within the articular cartilage, associated with secondary inflammatory factors¹. The temporomandibular joint (TMJ) plays an important role in craniofacial growth and function, and shows a high incidence of OA². TMJ is one of many synovial joints and data gathered from other synovial joints about OA can sometimes be applied to the TMJ³. However, each joint has its unique function, e.g., the knee joint is a load-bearing joint whereas TMJ is a shear-bearing joint⁴. OA lesions tend to develop mainly in old age in the knee joint^{5,6}, whereas OA lesions in the TMJ can be seen in relatively young patients and animals^{2,7,8}.

Articular cartilage is composed of ECM and chondrocytes. Chondrocytes, predominant in the cartilage of the TMJ, control the synthesis and degradation of articular ECM components³. Many studies had investigated the morpho-

logical and biochemical changes that occur during disease progression. Although several genes related to OA had been found, a comprehensive study of the gene expression profiles of osteoarthritic cartilage in the TMJ is still missing.

Microarray analysis is a powerful technique to study gene expression. This technique enables researchers to detect the relative concentration of thousands of transcripts in a single experiment and has become the most common approach for the study of gene functions, drug evaluation, pathway dissection and classification of clinical samples^{9–11}. Recently, researchers have used this technology to study gene expression during OA. Aigner *et al.* studied the anabolic and catabolic gene expression patterns in normal vs osteoarthritic cartilage using a cDNA array¹². Moreover, clusterin and beta-2 microglobulin were identified to be involved in OA pathogenesis using microarray analysis^{13,14}. This technology has also been applied to study the gene expression patterns of chondrocytes, *in vitro*^{15,16}. Spears *et al.* recently studied tumor necrosis factor (TNF) expression in adjuvant-induced arthritis in the TMJ with the use of a cDNA microarray containing 1148 genes. Samples from TMJ tissue (synovium, retrodiscal tissue and articular disc) were pooled to study the expression of TNF-alpha and its receptors in acute inflammation¹⁷. All these studies have shed light on the molecular mechanisms underlying OA and demonstrated the biological complexity of this disease. However, the

*Address correspondence and reprint requests to: Xuchen Ma, Center for TMD & Orofacial Pain, School of Stomatology, Peking University, 22 Zhongguancun South Street, Beijing 100081, PR China. Tel: 8610-62179977x2345; Fax: 8610-62173402; E-mail: kqxcma@bjmu.edu.cn

Received 20 November 2004; revision accepted 27 March 2005.

technology used in past studies limits the amount of progress made, in that they: (1) include finite numbers of representative gene probe sets on commercial microarrays, (2) are unable to detect splice variants, and (3) have a shortage of suitable data mining tools.

Our study has focused on identifying some novel candidate genes relating to OA. A comprehensive molecular profiling of OA progression is an important first step in discovering new candidate target molecules that are potentially involved in the pathogenesis of OA. In present study, Affymetrix RAE230A microarrays were used to simultaneously compare the expression of over 15,000 transcripts between rats with osteoarthritic cartilage of the TMJ and normal controls. We identified many novel genes that were differentially expressed in osteoarthritic cartilage. Some of these gene transcripts were further analyzed by quantitative real-time reverse transcriptase polymerase chain reaction (RT-PCR) to validate data gathered from the DNA microarray analysis. To the best of our knowledge, this study represents the first report of gene expression patterns in osteoarthritic cartilage in the TMJ using DNA microarray analysis.

Materials and methods

SURGICAL PROCEDURES

The study was performed in accordance with Peking University Animal Care Regulations. Two-month-old male Wistar rats (200–220 g) were anesthetized with sodium pentobarbital (50 mg/kg). To induce OA, lesions were created in the discs of the TMJ as described by Lekkas *et al.*¹⁸, with minor modifications. Under sterile surgical conditions, the left TMJ was exposed and one-third of the disc in the anterior and lateral regions of the joint was resected. The incision was then sutured and rats were given a normal diet for the remainder of the experiment. Age-matched rats with no surgical operation on both sides of TMJ were used as normal controls.

PATHOLOGICAL EXAMINATION

Rats were killed at 2, 4, 6, 8, or 12 weeks postoperatively with an overdose of sodium pentobarbital (> 70 mg/kg). The left condyles of the TMJs were removed and fixed in 4% paraformaldehyde in phosphate buffered salt solution (PBS) and demineralized in 15% EDTA. The specimens were dehydrated in graded alcohols and xylene, embedded in paraffin, and cut serially into 5- μ m sagittal sections. The sections were stained with hematoxylin–eosin and toluidine blue. The pathological conditions of OA were determined according to the histological criteria described by Dijkgraaf *et al.*¹.

TISSUE AND RNA PREPARATION

Two time points, 4 and 12 weeks postoperatively, were selected for studying the differential gene expression pattern of normal and osteoarthritic TMJ cartilage using DNA microarrays. Mandibular condyles were removed and condylar cartilage was carefully separated from the underlying bone, rapidly submerged in RNAlater (Qiagen) and stored at -20°C until RNA extraction. Total RNA was extracted using Trizol Reagent (Invitrogen Life Technologies) according to the manufacturer's instruction, after the cartilage samples were homogenized in liquid nitrogen with a pestle and a mortar. The RNA sample was further

purified with RNeasy Mini Column (Qiagen). The RNA concentration was evaluated by A260/A280 measurement and quality assessed by electrophoresis on a 1.0% agarose gel. Each RNA sample used for hybridization was extracted from 10 mandibular condyles to ensure adequate amount of tissue for RNA analysis and to decrease animal-to-animal variance. At per time point, we used three separate OA samples (30 rats), and three separate normal control samples (30 rats) for hybridization.

PROBE PREPARATION

Microarray hybridization probes, derived from isolated RNA samples, were generated in the following steps: reverse transcription of 10 μ g of total RNA was performed using an oligo (dT) primer containing T7 promoter (Operon) and SuperScript II reverse transcriptase (Invitrogen Life Technologies) in a reaction volume of 20 μ L to obtain first strand cDNAs. Second strand cDNAs were then synthesized in a total volume of 150 μ L. The double-stranded cDNA was purified using phenol chloroform and biotin-labeled cRNA was synthesized using Enzo RNA Transcript Labeling Kit (Affymetrix). *In vitro* transcription products were purified using RNeasy Columns, and biotinylated cRNA probes were fragmented.

HYBRIDIZATION

Biotinylated fragmented cRNA probes were hybridized in the microarray RAE230A (Affymetrix, Santa Clara, CA), which contained probe sets of over 15,000 known transcripts and expressed sequence tags (ESTs). Hybridization was performed at 45°C for 16 h in a hybridization oven (Affymetrix). The microarrays were then automatically washed and stained with streptavidin–phycoerythrin conjugate in an Affymetrix Genechip Fluidics Station. Fluorescence intensities were scanned with a GeneArray Scanner (Affymetrix). Hybridization was carried out independently, in triplicate, at each time point.

MICROARRAY DATA ANALYSIS

An Affymetrix Genechip Operating System 1.2 (GCOS1.2) was used to analyze the scanned image and to obtain and scale quantitative information (according to the Affymetrix Statistical Algorithms Reference Guide). Student's *t* tests (unpaired, two-tailed, unequal variance) were used to analyze and determine the significance of changes in the means of the following groups: control vs early-stage OA, control vs late-stage OA, and early-stage OA vs late-stage OA. The transcripts with *P*-values < 0.05 were selected for further analysis. A scaling signal intensity was generated for each probe using GCOS1.2 and triplicate scaling signal intensities from three independent experiments were then averaged to generate the average signal intensity (ASI) for each probe. Changes in intensity were then calculated.

In brief, differentially expressed genes in normal and different stages of OA were filtered according to the following criteria – (1) filter on *t* test: an unpaired *t* test was used to assess statistical significance, with a significance level of *P* < 0.05; (2) filter on signal: present in at least two of six samples in each comparison; (3) genes that were ≥ 2 -fold up- or down-regulated between any two groups were selected.

The selected genes were uploaded to Netaffx (<http://www.affymetrix.com>) for analysis and were annotated

according to gene ontology (GO) classifications¹⁹, which characterizes genes based on defined categories of molecular function, biological process, and cellular component.

CLUSTER ANALYSIS

A self-organizing map (SOM) was performed for the analysis and visualization of gene expression profiles based on differentially expressed genes using Affymetrix Data Mining Tool 3.0. Genes were then annotated using GO classifications.

QUANTITATIVE REAL-TIME RT-PCR ANALYSIS

Five differentially expressed genes were selected from the microarray results to further confirm the reliability of the array data. Total RNA was isolated using Trizol Reagent (Invitrogen Life Technologies) according to the manufacturer's protocol after cartilage samples were homogenized with a pestle and a mortar in liquid nitrogen. One microgram total RNA of normal or osteoarthritic cartilage was reverse transcribed to cDNA. Single-strand cDNA was synthesized with SuperScript II reverse transcriptase (Invitrogen Life Technologies). Quantitative real-time PCR was performed in Rotor-Gene 3000 (Corbett Research) with a Uniprimer™ in PCR by using S7901 Amplifluor™ Universal Amplification and Detection System (Chemicon) according to the manufacturer's instructions and the principle was described by Nuovo *et al.*²⁰. PCR was performed by mixing 2.5 μ L of 10 \times PCR buffer with 15 mM MgCl₂, 2.5 μ L of 2.5 mM dNTP, 2.5 μ L of 10 \times Z-tailed primer (0.5 μ M), 2.5 μ L of 10 \times untailed primer (5 μ M), 2.5 μ L of Amplifluor™ UniPrimer™, 0.25 μ L of *Taq* polymerase (5 units/ μ L), 10.25 μ L ddH₂O and 2.0 μ L DNA sample in 25 μ L reactions. Each experiment was done in triplicate. The expression levels of mRNA were normalized by the average expression of glyceraldehyde-3-phosphate dehydrogenase (GAPDH). The primer sets for the six genes were designed as presented in Table I.

STATISTICAL ANALYSIS

Data are presented as mean \pm standard error (S.E.), and comparisons between groups were performed using

Student's unpaired *t* test and considered to be significant if $P < 0.05$.

Results

PATHOLOGICAL EXAMINATION

Histological examination of mandibular condylar cartilage (MCC) in the postoperative rat demonstrated time-related progressive osteoarthritic changes. Normal cartilage had a smooth, intact superficial zone and no loss of proteoglycan staining in the mid- or deep zones, as determined by toluidine blue. In contrast, cartilage at 4 weeks postoperatively showed early-stage osteoarthritic changes, including swelling, superficial fibrillation and uneven proteoglycan staining. Cartilage at 6 and 8 weeks postoperatively demonstrated intermediate-stage osteoarthritic changes, including horizontal splitting, cluster formation and loss of proteoglycan staining. Cartilage at 12 weeks showed late-stage osteoarthritic changes, including extensive fibrillation, severely structural disorganization and extensive loss of proteoglycan staining (Fig. 1). Cartilage at two time points, 4 and 12 weeks postoperatively were selected to study the gene expression patterns during the progression of OA.

MICROARRAY DATA AND CLUSTER ANALYSIS

We compared gene expression profiles between normal and osteoarthritic TMJ cartilage using the Affymetrix oligonucleotide microarray technique. Among the 15,000 tested transcripts and ESTs, 1279 showed a statistical difference in expression. Of these 1279, 138 showed over a 2-fold change during the progression of OA. The information for each probe set on the RAE230A microarray was acquired in Netaffx (<http://www.affymetrix.com>, downloaded on January 12, 2005). Classification of the 138 strongly differentially expressed genes was performed according to the annotations of GO (<http://www.geneontology.org>, downloaded on January 12, 2005). Among the 138 genes, 76 have been sequenced at full-length and the others were ESTs. The genes with known sequences were classified according to GO, in terms of molecular function and biological process, and sorted by percentages according to Fatigo (<http://fatigo.bioinfo.cnio.es>), a web interface

Table I
Primer sets used for the quantitative real-time RT-PCR analysis*

Gene symbol	Primers (5'–3')	Product size (bp)	Annealing temperature (°C)
GAPDH	Forward <i>act gaa cct gac cgt aca</i> CAT GGC CTT CCG TGT TCC T	107	55.0
	Reverse CGC CTG CTT CAC CAC CTT CT		
NOV	Forward CGC CCT TCA ATA CCA AAA CCA	184	53.0
	Reverse <i>act gaa cct gac cgt aca</i> TTC CCT GGG CAC CTG TTA CAT		
EGLN3	Forward <i>act gaa cct gac cgt aca</i> CCC CAT GGC TCT GTT TTG TTT	121	53.0
	Reverse TCC CTG CCT TCG TTG TGT TTA		
MMP3	Forward TGG AAG GCG TCG TGT GTT T	108	54.0
	Reverse <i>act gaa cct gac cgt aca</i> CTC CCA TTT TGC TCT GCC ATA		
AQP3	Forward ACC CAG GAG TGC GTT TCT AAG TA	174	54.0
	Reverse <i>act gaa cct gac cgt aca</i> GCC CCT CCC AAT GTC TAT CTT		
DKK3	Forward CAG GGA GGG TAT GGC GTT AGA	102	53.0
	Reverse <i>act gaa cct gac cgt aca</i> AAG GGA AAG AGG GAG AAA GCT		

*One primer is designed to contain target-specific sequences plus the Z sequence at the 5' end (Z-tailed primer), and the other primer contains only target-specific sequences (untailed primer). Z sequence: *act gaa cct gac cgt aca*. The UniPrimer™ consists of a 3' oligonucleotide tail (Z sequence) and 5' intra-complementary sequence labeled with a pair of energy transfer molecules.

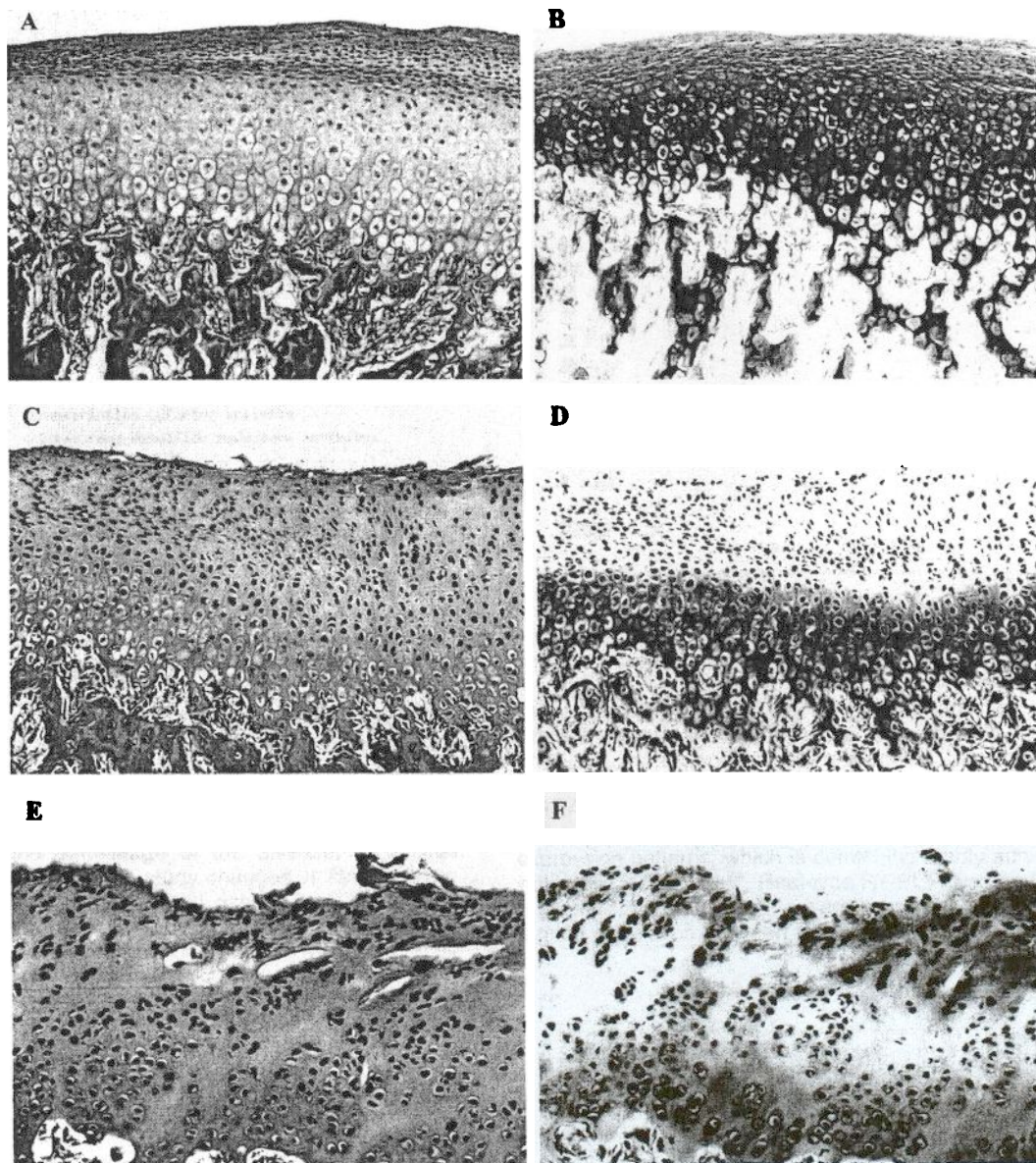


Fig. 1. Pathological examinations of MCCs postoperatively and normal controls. A, B: A smooth, intact superficial zone and no loss of proteoglycan staining in the mid- or deep zones are visible in normal adult cartilage. C, D: Cartilage at 4 weeks postoperatively showed swelling, superficial fibrillation and uneven proteoglycan staining. E, F: Cartilage at 12 weeks postoperatively showed extensive fibrillation, severely structural disorganization and extensive loss of proteoglycan staining throughout the mid- and deep zone. (A, C, E: hematoxylin-eosin staining $\times 100$; B, D, F: toluidine blue staining $\times 100$).

which carries out data mining using GO for DNA microarray data²¹ (Figs. 2 and 3).

SOM is an unsupervised, neural network learning algorithm which has been successfully used for the analysis and organization of large data files²². This clustering algorithm allows for the separation of distinct patterns of expression based on the similarity of expression profiles between different genes. SOM clustering analysis of the 138 altered genes revealed four unique patterns of gene expression (Fig. 4), and these genes were grouped into four clusters (clusters 1–4). Gene expression ratios of 138 transcripts in different clusters are shown in Tables II–V.

QUANTITATIVE REAL-TIME RT-PCR ANALYSIS

To further validate the results of the microarray analysis, five genes having over 2-fold changes in microarray analysis were selected for confirmation by using quantitative real-time RT-PCR analysis. The expression levels of mRNA were normalized by the average expression of GAPDH and the results are shown in Fig. 5. The mRNA expression of MMP3, AQP3, NOV, DKK3, and EGLN3 were analyzed by quantitative PCR and revealed a similar expression pattern to microarray results, demonstrating a good correlation between the two methods.

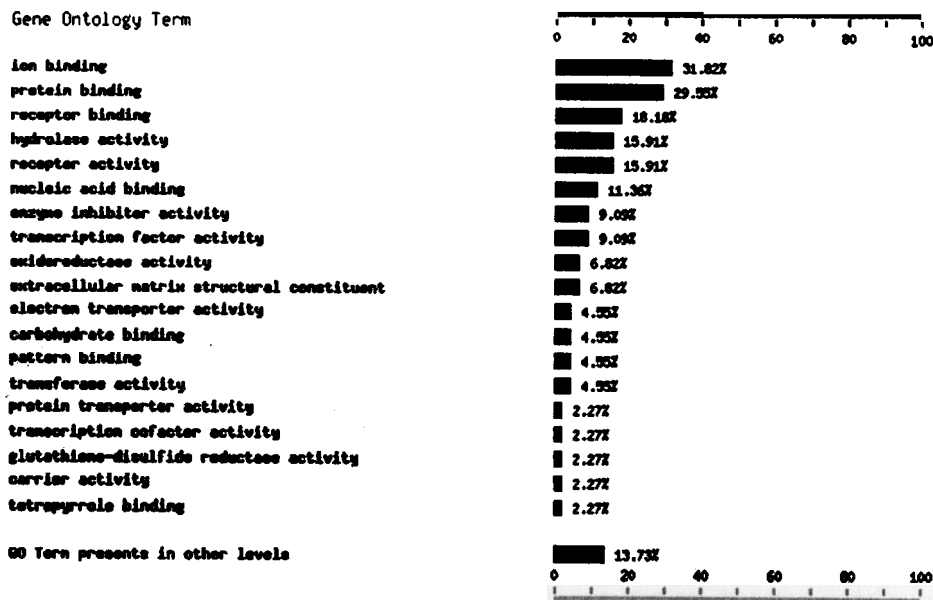


Fig. 2. Classification of molecular functions. The differentially expressed genes with a ≥ 2 -fold change in the progression of OA were classified according to molecular functions of GO annotations. FatGO extract GO terms annotated for these genes sorting by percentages (level = 3). Percentages are calculated with respect to only those genes that have been GO annotated.

Discussion

The current study was performed directly on MCC, which can better represent the osteoarthritic state *in vivo* than isolated chondrocyte, synovial fluid, or cultured explants. Because of scarce availability of human TMJ cartilage, especially in the early-stage of the disease, an animal model has been created to study changes of TMJ cartilage in different stages of OA and to assess new therapeutic strategies. In the present study, we induced experimental OA in the TMJ based on surgical procedures described by

Lekkas²³ and confirmed OA by pathological examination. While there are some drawbacks to using a DNA microarray, e.g., missing post-transcriptional regulation and post-translational modifications or incomplete relevance of mRNA level vs protein level, the technique provides a powerful tool for obtaining an overview of gene expression patterns, which is something hardly achievable with other techniques²⁴. Real-time RT-PCR was performed to confirm the results of microarray analysis and revealed a good correlation between these two methods.

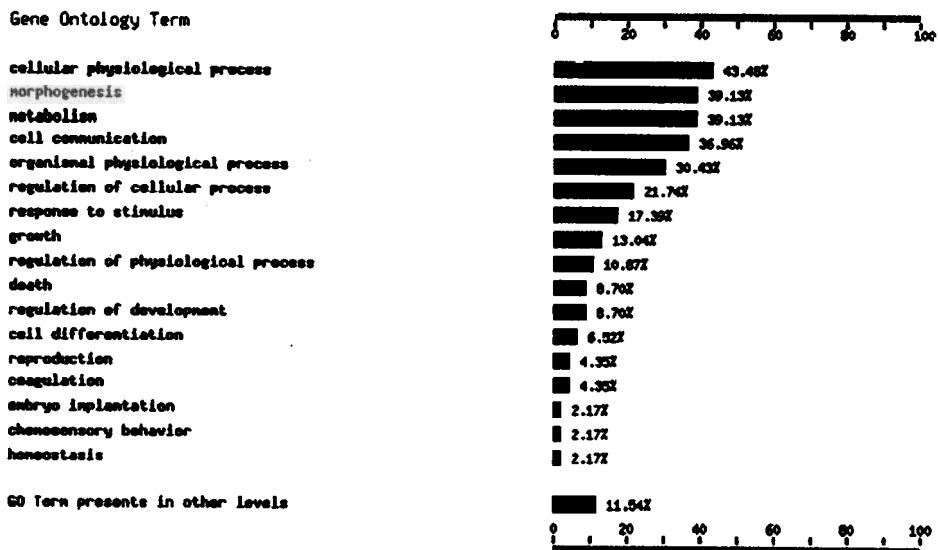


Fig. 3. Classification of biological processes. The differentially expressed genes with a ≥ 2 -fold change in the progression of OA were classified according to the biological processes of GO annotations. FatGO extract GO terms annotated for these genes sorting by percentages (level = 3). Percentages are calculated with respect to only those genes that have been GO annotated.

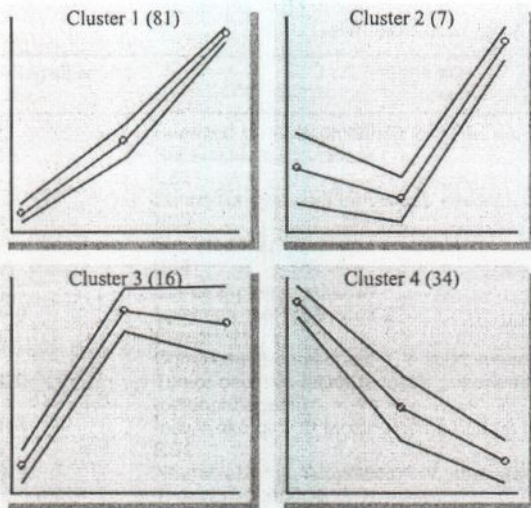


Fig. 4. SOM clustering analysis. One hundred and thirty-eight differentially expressed genes were grouped into four clusters according to SOM clustering algorithm. X- and Y-axes represent time point and relative expression levels, respectively. From left to right, the first point shows normal control values, the second point shows early-stage OA expression levels, and the final point shows late-stage OA expression levels. Each of the four clusters demonstrated a unique pattern of expression based on the similarity of the expression pattern of its constituent genes. The number of transcripts in each cluster is shown in parenthesis.

By using microarray techniques, we compared gene expression profiles between normal and osteoarthritic TMJ cartilage in rats. According to GO annotations, these genes spanned many members of distinct functional families, including ion binding, protein binding, nucleic acid binding, receptor activity, hydrolase activity, enzyme inhibitor activity, transcription factor activity, oxidoreductase activity and structural molecule activity. These genes also encompassed many biological processes, including metabolism, morphogenesis, cell growth and death, cell communication, regulation of development and cell differentiation.

SOM analysis of the 138 genes revealed four unique patterns, or clusters, of gene expression (Fig. 4). Cluster 1 included 81 transcripts which had continuous elevation from early to late-stage OA, suggesting that these genes may play roles during the entire progression of OA. Cluster 1 included many known genes, such as MMP3, SPIN2C, PLAT, CHAD, TNFRSF11B, CLU, SFRP4 and HIG1 which have been shown to be associated with OA^{13,14,25}. In addition, some new genes and ESTs which haven't been previously been associated with OA, were also included in this cluster. Cluster 2 contained 7 transcripts which showed little or no down-regulation in early-stage OA and then a dramatic up-regulation in late-stage OA. This cluster mainly consisted of ESTs. However, member 11 of the tumor necrosis factor ligand superfamily member (TNFSF 11), an osteoclast differentiation factor which induces osteoclast formation and bone resorption²⁶, appeared to be up-regulated in late-stage OA. Thus, it may be involved in bone resorption in late-stage OA. Cluster 3 included 16 transcripts, which rapidly increased and almost peaked at the early-stage time point, which suggests that these genes may play roles in the initiation of OA, and may thus be used as markers of early-stage OA. The high expression of TIMP3 and GSR within this cluster suggests a protective

effect in early-stage of OA. However, the molecular functions of most of the transcripts in this cluster are still not clear according to GO classification and their relations to OA need to be further studied. Cluster 4 included transcripts which were continuously down-regulated during OA progression. The most striking inhibition was observed in chondromodulin-1 (CHM-1), a cartilage derived anti-angiogenic factor, which has been shown to regulate vascular invasion during endochondral bone formation. CHM-1, which is highly expressed in articular cartilage, plays a role in the maintenance of avascularity of normal cartilage. Thus, decreased levels of CHM-1 might be partially responsible for promoting blood vessel invasion into the cartilage during OA^{27,28}. Bone morphogenetic proteins (BMPs) induce cartilage and bone formation²⁹, and the down-regulation of BMP1 and BMP3 may be related to the disorders of cartilage and bone formation during OA.

After integrating information from GO classifications and SOM clustering analysis, there appears to be a series of very complicated molecular events that contribute to OA progression. Each unique SOM pattern included transcripts from different classifications. In cluster 1, the up-regulated genes not only included genes related to proteolysis like MMP3, PLAT and C1S, but also some apoptosis-related genes, like TNFRSF11B, EGLN3 and CLU. Moreover, increased IGFBP5 and IGFBP6 expressions in cluster 1 may block IGF-I activity and potentially inhibit the anabolic activities of chondrocytes³⁰. Down-regulation of BMP1 and BMP3 in cluster 4 and imbalance of TNFSF11 (cluster 2) and TNFRSF11B (cluster 1) may cooperate in the damage of bone and cartilage during OA. Interestingly, though, genes in the same classification sometime had different expression levels. For example, the enzyme inhibiting activity of SERPINA1, SPIN2C and SPP2 (cluster 1) continuously increased, but A2M, a wide-spectrum protease inhibitor significantly decreased (cluster 4), and TIMP3 increased and peaked in early-stage (cluster 3). The mechanisms governing these changes are not clear, but considering the high expression of proteinases in cluster 1, it's possible that a balance between the proteinase and its inhibitor was disturbed. This balance may play an important role in the pathogenesis of OA.

In the present study, a widespread differential gene expression profile was made in OA progression, as mentioned above. Many of these genes have been previously demonstrated to be associated with OA, and more importantly, we have uncovered numerous new genes and ESTs which have never been related to OA. However, it should be noted that only transcripts ≥ 2 -fold change in expression were selected, some important genes that are expressed or repressed during OA progression might have been missed in this study. Although our main focus was on cluster 1, the biggest of the four clusters, and the validation of genes was performed mainly from this cluster, the other clusters may be equally important during OA progression. Additionally, some ESTs may play potential roles in OA. Thus, further studies are needed.

Aquaporins (AQPs) are integral membrane proteins that serve as channels for water transport across the membrane. A recent report showed that AQP1 was expressed in articular chondrocytes and up-regulated in rheumatoid arthritis (RA)³¹. Additionally, AQP3 was expressed in normal equine articular chondrocytes³². Although AQP1–9 genes are present on the microarray of RAT230A, only AQP1, AQP3 and AQP6 were expressed in MCC in the present study. AQP3 mRNA was highly up-regulated in OA

Table II
Gene expression ratios of 81 transcripts in cluster 1

Genebank identifier	Gene title	Gene symbol	EOA vs CO	LOA vs CO
BI291181	Secreted phosphoprotein 2, 24 kDa	Spp2	19.0	32.0
NM_012880	Superoxide dismutase 3	Sod3	3.7	9.6
BI290821	EST	—	3.0	7.4
NM_022519	Serine (or cysteine) proteinase inhibitor, clade A, member 1	Serpina1	2.0	6.9
AI599143	EST	—	3.2	6.8
AF140346	Secreted frizzled-related protein 4	Sfrp4	2.0	6.2
BG373119	EST	—	2.2	6.0
NM_031531	Serine protease inhibitor	Spin2c	3.6	5.9
NM_017149	Mesenchyme homeobox 2	Meox2	2.6	5.2
BG673439	Claudin 11	Cldn11	2.6	5.1
D88250	Complement component 1, s subcomponent	C1s	2.6	4.9
NM_012870	Tumor necrosis factor receptor superfamily, member 11b (osteoprotegerin)	Tnfrsf11b	2.9	4.9
NM_013104	Insulin-like growth factor-binding protein 6	Igfbp6	2.3	4.8
BM388957	EST	—	3.1	4.7
NM_031609	Neuroblastoma, suppression of tumorigenicity 1	Nb11	2.0	4.6
X89963	Thrombospondin 4	Thbs4	2.7	4.6
AF109674	Late gestation lung protein 1	Lg11	1.6	4.6
NM_019164	Chondroadherin	Chad	2.8	4.5
M25804	Nuclear receptor subfamily 1, group D, member 1	Nr1d1	2.2	4.5
AI011747	Proline arginine-rich end leucine-rich repeat protein	Prlep	2.7	4.5
BG673588	Insulin-like growth factor binding protein 6	Igfbp6	2.1	4.4
NM_016996	Calcium-sensing receptor	Casr	1.6	4.3
AF314657	Clusterin	Clu	1.8	4.2
AI411941	EST	—	2.4	4.2
AI175861	Late gestation lung protein 1	Lg11	1.4	4.0
U23407	Cellular retinoic acid binding protein 2	Crabp2	2.0	3.9
NM_133523	Matrix metalloproteinase-3	Mmp3	2.5	3.6
NM_031556	Caveolin	Cav	2.1	3.6
NM_022270	Organic cation transporter OCTN1	Octn1	2.4	3.5
AI716243	EST	—	2.3	3.3
NM_017254	5-Hydroxytryptamine (serotonin) receptor 2A	Htr2a	2.0	3.2
BF418649	EST	—	1.6	3.2
AI410438	EST	—	1.3	3.1
AB071036	Leucine-rich repeat protein induced by beta-amyloid	Lib	1.9	3.1
NM_021576	5 Nucleotidase	Nt5	1.8	3.0
BI281230	EST	—	1.7	3.0
AF347936	Interleukin 11 receptor, alpha chain 1	Il11ra1	1.4	3.0
BE104060	Insulin-like growth factor-binding protein 5	Igfbp5	1.4	2.9
NM_031703	Aquaporin 3	Aqp3	1.8	2.9
BI285449	Caveolin	Cav	1.9	2.9
BI278545	Dermatopontin	Dpt	2.0	2.8
BI285485	Dermatopontin	Dpt	1.9	2.8
BG379319	Transforming growth factor, beta induced, 68 kDa	Tgfb1	2.2	2.7
NM_012636	Parathyroid hormone-like peptide	Pthlh	2.1	2.7
BI292028	Guanine deaminase	Gda	2.1	2.7
BM390827	EST	—	1.7	2.7
NM_019371	EGL nine homolog 3 (<i>C. elegans</i>)	Egln3	2.0	2.7
AF245040	Dickkopf homolog 3 (<i>Xenopus laevis</i>)	Dkk3	1.6	2.7
BM387419	EST	—	1.5	2.6
AI406412	EST	—	1.4	2.6
BI285086	EST	—	1.6	2.6
NM_133569	Angiopietin-like 2	Angpt12	2.0	2.5
AA819776	Heat shock protein 1, alpha	Hspca	1.6	2.5
BF551311	EST	—	1.7	2.5
AA965084	EST	—	1.7	2.5
U44948	Cysteine and glycine-rich protein 2	Csrp2	1.9	2.5
AF245172	Guanine deaminase	Gda	2.0	2.5
AI010863	EST	—	1.4	2.4
NM_030868	NOV protein	Nov	1.6	2.4
NM_033499	Scrapie responsive gene 1	Scrg1	1.7	2.4
AI600037	EST	—	1.8	2.4
BE113700	Paired related homeobox 2	Prrx2	1.2	2.4
NM_080698	Fibromodulin	Fmod	1.9	2.4
BI296216	EST	—	1.4	2.4
BG671589	EST	—	1.4	2.4
AI233530	EST	—	1.3	2.4

(continued on next page)

Table II (continued)

Genebank identifier	Gene title	Gene symbol	EOA vs CO	LOA vs CO
NM_013151	Plasminogen activator, tissue	Plat	1.2	2.3
H31665	Hypoxia induced gene 1	Hig1	1.4	2.3
J04035	Elastin	Ein	1.7	2.2
AA963797	EST	—	1.5	2.2
BM389225	Angiopoietin-like 2	Angpt12	1.8	2.2
BM384570	EST	—	1.5	2.2
AA892549	EST	—	1.4	2.1
BM389611	EST	—	1.4	2.1
AA892234	EST	—	1.4	2.1
AA875017	EST	—	1.2	2.1
BI276341	EST	—	1.2	2.1
BI292351	EST	—	1.4	2.1
NM_022290	Tenomodulin	Tnmd	1.7	2.1
AI102401	EST	—	1.4	2.1
AB073318	Brain and acute leukemia, cytoplasmic	Balc	1.2	2.0

EOA vs CO: early-stage OA vs control; LOA vs CO: late-stage OA vs control. List sorted according to the fold change of LOA vs CO in descending order.

Table III
Gene expression ratios of seven transcripts in cluster 2

Genebank identifier	Gene title	Gene symbol	EOA vs CO	LOA vs CO
NM_022242	Niban protein	Niban	1.0	2.5
AA963085	EST	—	0.9	2.3
BF406261	Similar to fatty acid transport protein 3	—	1.0	2.2
NM_057149	Tumor necrosis factor (ligand) superfamily, member 11	Tnfsf11	1.1	2.0
BI275179	EST	—	0.8	2.0
BF400611	EST	—	0.8	2.0
BI287026	EST	—	0.7	2.0

EOA vs CO: early-stage OA vs control; LOA vs CO: late-stage OA vs control. List sorted according to the fold change of LOA vs CO in descending order.

Table IV
Gene expression ratios of 16 transcripts in cluster 3

Genebank identifier	Gene title	Gene symbol	EOA vs CO	LOA vs CO
BM383043	Similar to hypothetical protein 4933417N17	—	4.8	4.1
925924	Similar to cytokine receptor like molecule 3	LOC290655	3.7	3.3
AI717113	Coagulation factor 5	F5	3.3	3.2
BI298356	Four and a half LIM domains 1	Fh11	2.8	2.9
BG673187	Four and a half LIM domains 1	Fh11	2.6	2.2
BG380282	Crystallin, alpha c	Cryac	2.4	2.4
AW520914	Calsequestrin 2	Casq2	2.3	2.5
AI599265	Tissue inhibitor of metalloproteinase-3	Timp3	2.3	2.1
NM_053906	Glutathione reductase	Gsr	2.2	1.6
BI285456	Granulosa cell HMG-box protein 1	Gcx-1	2.1	2.6
AI237401	EST	—	2.1	2.0
AI406795	EST	—	2.1	2.5
AI549393	EST	—	2.1	2.1
BI289517	EST	—	2.0	1.8
AI235906	Similar to protein phosphatase 2C epsilon	LOC3 10506	2.0	2.1
BI300986	EST	—	1.9	2.3

EOA vs CO: early-stage OA vs control; LOA vs CO: late-stage OA vs control. List sorted according to the fold change of EOA vs CO in descending order.

Table V
Gene expression ratios of 34 transcripts in cluster 4

Genebank identifier	Gene title	Gene symbol	EOA vs CO	LOA vs CO
NM_030854	Chondromodulin-1	Chm-1	0.2	0.1
BF284168	H19 fetal liver mRNA	H19	1.0	0.2
AI408151	EST	—	0.4	0.2
NM_012488	Alpha-2-macroglobulin	A2m	0.5	0.3
NM_019348	Somatostatin receptor 2	Sstr2	1.0	0.3
NM_012760	Pleiomorphic adenoma gene-like 1	Plag11	0.4	0.3
AI102732	EST	—	0.8	0.3
AI639162	EST	—	0.8	0.4
AA891634	EST	—	0.4	0.4
NM_017105	Bone morphogenetic protein 3	Bmp3	0.6	0.4
BF289017	EST	—	0.8	0.4
BF285466	EST	—	0.5	0.4
AI009713	EST	—	0.6	0.4
AB012139	Bone morphogenetic protein 1	Bmp1	0.6	0.5
BI285551	Similar to hypothetical protein FLJ12442	—	0.7	0.5
AA892497	Xylosyltransferase II	Xy1t2	1.0	0.5
NM_017058	Vitamin D receptor	Vdr	0.7	0.5
NM_031333	Cadherin 2	Cdh2	0.6	0.5
U73184	Syndecan 3	Sdc3	0.6	0.5
AI071102	EST	—	0.5	0.5
BI279363	EST	—	0.6	0.5
AI230228	Phosphoserine aminotransferase 1	Psat1	0.6	0.5
AA800908	EST	—	0.7	0.5
BE098713	EST	—	0.5	0.5
AA964250	EST	—	0.7	0.5
AW252428	EST	—	0.7	0.5
BM384604	Similar to phosphoenolpyruvate carboxykinase 2	—	0.7	0.5
BI282755	EST	—	0.6	0.5
AI407489	Matrin F/G 1	Matr1	0.7	0.5
BM391851	EST	—	0.6	0.5
BM386525	EST	—	0.5	0.5
BI298526	EST	—	0.2	0.6
BG671786	EST	—	0.5	0.6
AW144216	Aminopeptidase A	Enpep	0.5	0.7

EOA vs CO: early-stage OA vs control; LOA vs CO: late-stage OA vs control. List sorted according to the fold change of LOA vs CO in ascending order.

cartilage, whereas there was no significant difference in expression of AQP1 or AQP6 between OA and normal controls. Over 70% of the total tissue weight in the cartilage matrix consists of water and osteoarthritic cartilage in early-stage OA is characterized by swelling with increased water content¹. Therefore water transport in the movement of cartilage matrix and metabolic water across the membranes of chondrocytes may be important in normal and pathological conditions of cartilage. The high expression of AQP3 in OA cartilage suggests that it may play a particular role in OA pathogenesis, but the mechanisms underlying this role require further study.

Secreted phosphoprotein 2 (SPP2), a 24 kDa non-collagenous protein, is a member of the cystatin superfamily, which may modulate the thiol protease activities that are known to be involved in bone turnover³³. SPP2 has been shown to be expressed in liver and bone, and also been identified as a component of the fetuin—mineral complex and may play a role in inhibiting calcification³⁴. SPP2 was the most striking changed gene in the present study, being up-regulated 19-fold in early-stage OA and 32-fold in late-stage OA. Although the expression of cysteine proteinases and their inhibitor, cystatin, in articular cartilage has been studied extensively in OA, no direct correlation has been reported between SPP2 and OA. Therefore, further study is required to uncover its possible role in OA pathogenesis.

The present work is the first to link Dickkopf 3 (DKK3) with OA progression. DKK3 is a member of the DKK family which act as Wnt signaling regulators by inhibiting the Wnt signaling pathway³⁵. It has never been reported to be

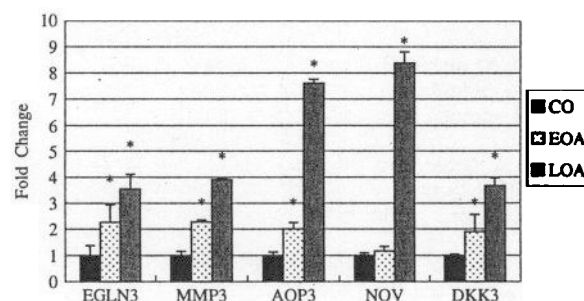


Fig. 5. Quantitative real-time RT-PCR analysis. Real-time RT-PCR analysis of the selected differentially expressed genes from the microarray results, and assays were performed in triplicate for each gene. Data are presented as fold changes when comparing osteoarthritic cartilage vs normal cartilage. CO: normal control. EOA: early-stage osteoarthritic cartilage. LOA: late-stage osteoarthritic cartilage. Values represent means with error bars. * $P < 0.05$.

expressed in cartilage. However, in the present study, there was high expression of DKK3 in OA cartilage. Secreted frizzled-related protein 4 (SFRP4), another inhibitor of the Wnt signaling pathway, was also strongly up-regulated in OA cartilage. SFRP4 inhibits Wnt action by competitively binding to the Wnt ligand and was expressed in human chondrocytes during severe OA¹⁴. Since the Wnt/frizzled members influence cell proliferation, differentiation and apoptosis³⁶, the over-expression of DKK3 and SFRP4 suggests that Wnt signaling pathways may play a role in the pathogenesis of OA.

NOV protein (NOV), a member of the CCN family, participates in angiogenesis, chondrogenesis, and osteogenesis. All these processes are likely to be involved in the control of cell proliferation and differentiation³⁷. It has been shown that NOV is expressed in the cartilage neoplasia and hypertrophic chondrocytes of growth plates in embryonic murine³⁸. In the present study, strong up-regulation of NOV was detected in OA cartilage, suggesting that NOV might play a role in maintenance of specific cartilage functions or repair of cartilage during OA progression. EGL nine homolog 3 (EGLN3) has been implicated in the regulation of growth, differentiation and apoptosis in muscle and nerve cells³⁹ and may promote caspase-dependent cell death. Given the possibility that NOV and EGLN3 might be involved in chondrocyte growth and apoptosis, further research is needed to explore their possible roles in OA pathogenesis.

In conclusion, the present study has provided a new and comprehensive expression profile of a large number of genes during the progression of OA by using unbiased DNA microarray quantitative analysis. Further investigation of the precise functional roles of these genes during OA will provide new insights in understanding the molecular mechanisms of this disease and pave the way for new therapeutic strategies and drug discovery.

Acknowledgments

We thank Ge Chen, Dengcheng Wu, Lu Sun for technical assistance, Junming Wang and Xiaoming Ou for review. This research was supported by the National Natural Science Foundation of China (Grant Number: 30371543, 30171015).

References

- Dijkgraaf LC, de Bont LG, Boering G, Liem RS. The structure, biochemistry, and metabolism of osteoarthritic cartilage: a review of the literature. *J Oral Maxillofac Surg* 1995;53:1182–92.
- Okeson JP. *Management of Temporomandibular Disorders and Occlusion*. 5th edn. St. Louis: Mosby, Inc. 2003;151–8.
- Dijkgraaf LC, de Bont LG, Boering G, Liem RS. Normal cartilage structure, biochemistry, and metabolism: a review of the literature. *J Oral Maxillofac Surg* 1995;53:924–9.
- Gepstein A, Shapiro S, Arbel G, Lahat N, Livne E. Expression of matrix metalloproteinases in articular cartilage of temporomandibular and knee joints of mice during growth, maturation, and aging. *Arthritis Rheum* 2002;46:3240–50.
- Peat G, McCamey R, Croft P. Knee pain and osteoarthritis in older adults: a review of community burden and current use of primary health care. *Ann Rheum Dis* 2001;60:91–7.
- Felson DT, Zhang Y, Hannan MT, Naimark A, Weissman BN, Aliabadi P. The incidence and natural history of knee osteoarthritis in the elderly. The Framingham Osteoarthritis Study. *Arthritis Rheum* 1995;38:1500–5.
- Stewart CL, Standish SM. Osteoarthritis of the TMJ in teenaged females: report of cases. *J Am Dent Assoc* 1983;106:638–40.
- Livne. Matrix synthesis in mandibular condylar cartilage of aging mice. *Osteoarthritis Cartilage* 1994;2:187–97.
- DeRisi J, Penland L, Brown PO, Bittner ML, Meltzer PS, Ray M, *et al.* Use of a cDNA microarray to analyse gene expression patterns in human cancer. *Nat Genet* 1996;14:457–60.
- Lockhart DJ, Dong H, Byrne MC, Follettie MT, Gallo MV, Chee MS, *et al.* Expression monitoring by hybridization to high-density oligonucleotide arrays. *Nat Biotechnol* 1996;14:1675–80.
- Golub TR, Slonim DK, Tamayo P, Huard C, Gaasenbeek M, Mesirov JP, *et al.* Molecular classification of cancer: class discovery and class prediction by gene expression monitoring. *Science* 1999;286:531–7.
- Aigner T, Zien A, Gehrsitz A, Gebhard PM, McKenna L. Anabolic and catabolic gene expression pattern analysis in normal versus osteoarthritic cartilage using complementary DNA-array technology. *Arthritis Rheum* 2001;44:2777–89.
- Connor JR, Kumar S, Sathie G, Mooney J, O'Brien SP, Mui P, *et al.* Clusterin expression in adult human normal and osteoarthritic articular cartilage. *Osteoarthritis Cartilage* 2001;9:727–37.
- Zhang H, Liew CC, Marshall KW. Microarray analysis reveals the involvement of beta-2 microglobulin (B2M) in human osteoarthritis. *Osteoarthritis Cartilage* 2002;10:950–60.
- Stokes DG, Liu G, Coimbra IB, Piera-Velazquez S, Crowl RM, Jimenez SA. Assessment of the gene expression profile of differentiated and dedifferentiated human fetal chondrocytes by microarray analysis. *Arthritis Rheum* 2002;46:404–19.
- Vincenti MP, Brinckerhoff CE. Early response genes induced in chondrocytes stimulated with the inflammatory cytokine interleukin-1beta. *Arthritis Res* 2001;3:381–8.
- Spears R, Oakes R, Moore C, Bellinger LL, Hutchins B. A determination of tumor necrosis factor expression in TMJ inflammation with the use of microarray analysis. *J Dent Res* 2003;82:807–13.
- Lekkas C, Honee GL, van den Hooff A. Effects of experimental defects of the articular disc of the temporomandibular joint in rats. *J Oral Rehabil* 1988;15:141–8.
- Ashburner M, Ball CA, Blake JA, Botstein D, Butler H, Cherry JM, *et al.* Gene ontology: tool for the unification of biology. The Gene Ontology Consortium. *Nat Genet* 2000;25:25–9.
- Nuovo GJ, Hohman RJ, Nardone GA, Nazarenko IA. *In situ* amplification using universal energy transfer-labeled primers. *J Histochem Cytochem* 1999;47:273–80.
- Al-Shahrour F, Diaz-Uriarte R, Dopazo J. FatiGO: a web tool for finding significant associations of gene

- ontology terms with groups of genes. *Bioinformatics* 2004;20:578–80.
22. Toronen P, Kolehmainen M, Wong G, Castren E. Analysis of gene expression data using self-organizing maps. *FEBS Lett* 1999;451:142–6.
 23. Lekkas C. Experimental degenerative temporomandibular joint disease. *Int J Oral Maxillofac Surg* 1994;23:423–4.
 24. Aigner T, Bartnik E, Zien A, Zimmer R. Functional genomics of osteoarthritis. *Pharmacogenomics* 2002;3:635–50.
 25. Coimbra IB, Jimenez SA, Hawkins DF, Piera-Velazquez S, Stokes DG. Hypoxia inducible factor-1 alpha expression in human normal and osteoarthritic chondrocytes. *Osteoarthritis Cartilage* 2004;12:336–45.
 26. Komuro H, Olee T, Kuhn K, Quach J, Brinson DC, Shikhman A, *et al.* The osteoprotegerin/receptor activator of nuclear factor kappaB system in cartilage. *Arthritis Rheum* 2001;44:2768–76.
 27. Shukunami C, Hiraki Y. Role of cartilage-derived anti-angiogenic factor, chondromodulin-I, during endochondral bone formation. *Osteoarthritis Cartilage* 2001;9(Suppl A):S91–S101.
 28. Hayami T, Funaki H, Yaoeda K, Mitui K, Yamagiwa H, Tokunaga K, *et al.* Expression of the cartilage derived anti-angiogenic factor chondromodulin-I decreases in the early stage of experimental osteoarthritis. *J Rheumatol* 2003;30:2207–17.
 29. Tabas JA, Zasloff M, Wasmuth JJ, Emanuel BS, Altherr MR, McPherson JD, *et al.* Bone morphogenetic protein: chromosomal localization of human genes for BMP1, BMP2A, and BMP3. *Genomics* 1991;9:283–9.
 30. Martel-Pelletier J, Di Battista JA, Lajeunesse D, Pelletier JP. IGF/IGFBP axis in cartilage and bone in osteoarthritis pathogenesis. *Inflamm Res* 1998;47:90–100.
 31. Trujillo E, Gonzalez T, Marin R, Martin-Vasallo P, Marples D, Mobasheri A. Human articular chondrocytes, synoviocytes and synovial microvessels express aquaporin water channels; upregulation of AQP1 in rheumatoid arthritis. *Histol Histopathol* 2004;19:435–44.
 32. Mobasheri A, Trujillo E, Bell S, Carter SD, Clegg PD, Martin-Vasallo P, *et al.* Aquaporin water channels AQP1 and AQP3, are expressed in equine articular chondrocytes. *Vet J* 2004;168:143–50.
 33. Hu B, Coulson L, Moyer B, Price PA. Isolation and molecular cloning of a novel bone phosphoprotein related in sequence to the cystatin family of thiol protease inhibitors. *J Biol Chem* 1995;270:431–6.
 34. Price PA, Nguyen TM, Williamson MK. Biochemical characterization of the serum fetuin–mineral complex. *J Biol Chem* 2003;278:22153–60.
 35. Kawano Y, Kypta R. Secreted antagonists of the Wnt signalling pathway. *J Cell Sci* 2003;116(Pt 13):2627–34.
 36. Chen S, Guttridge DC, You Z, Zhang Z, Fribley A, Mayo MW, *et al.* Wnt-1 signaling inhibits apoptosis by activating beta-catenin/T cell factor-mediated transcription. *J Cell Biol* 2001;152:87–96.
 37. Perbal B. CCN proteins: multifunctional signaling regulators. *Lancet* 2004;363:62–4.
 38. Yu C, Le AT, Yeger H, Perbal B, Alman BA. NOV (CCN3) regulation in the growth plate and CCN family member expression in cartilage neoplasia. *J Pathol* 2003;201:609–15.
 39. Taylor MS. Characterization and comparative analysis of the EGLN gene family. *Gene* 2001;275:125–32.